EUMETSAT OSI SAF
OCEAN AND SEA ICE

Algorithm Theoretical Baseline Document for Atlantic High Latitudes level 3 Radiative Flux products

OSI-301-c and OSI-302-c

Version: 1.2

Date: 05/11/2022

Øystein Godøy

Steinar Eastwood

Atle Sørensen

Norwegian Meteorological Institute

Document versions and Changes record

Document version	Software version	Date	Author	Change description
1.0		14-04-2011	Øystein Godøy	
1.1-draft	5.3	05-12-2019	Amélie Neuville	Document reorganisation. Changes corresponding to the new product versions OSI-301-b and OSI-302-b
1.1	5.3	12-02-2020	Steinar Eastwood	Minor changes after ORR review
1.2	5.4	05-11-2022	Steinar Eastwood	Updates for new product version OSI-301-c and OSI-302-c, added correction of VIIRS data, change in cloudy sky parametrization.

Table of contents

1. Introduction

1.1. The EUMETSAT Ocean and Sea Ice SAF

The Satellite Application Facilities (SAFs) are dedicated centres of excellence for processing satellite data – hosted by a National Meteorological Service – which utilise specialist expertise from institutes based in Member States. EUMETSAT created Satellite Application Facilities (SAFs) to complement its Central Facilities capability in Darmstadt. The Ocean and Sea Ice Satellite Application Facility (OSI SAF) is one of eight EUMETSAT SAFs, which provide users with operational data and software products. More on SAFs can be read at www.eumetsat.int.

The objective of the OSI SAF is the operational near real-time production and distribution of a coherent set of information, derived from earth observation satellites, and characterising the ocean surface and the energy fluxes through it: sea surface temperature, radiative fluxes, wind vector and sea ice characteristics. For some variables, the OSI SAF is also aiming at providing long term data records for climate applications, based on reprocessing activities.

The radiative fluxes products includes longwave and shortwave downward irradiance at the surface. The longwave product is labelled Downward Longwave Irradiance (DLI) product, with identifier OSI-301-c. The shortwave product is labelled Surface Shortwave Irradiance (DLI) product, with identifier OSI-302-c.

The OSI SAF consortium is hosted by Météo-France. The high latitude radiative processing is performed at the High Latitude processing facility (HL centre), under the responsibility of the Norwegian Meteorological Institute.

1.2. Disclaimer

Note: The comments that we get from our users are important inputs when defining development activities and updates, and user feedback to the OSI SAF project team is highly valued.

Acknowledgement and citation

Use of these products should be acknowledged with the following citations:

OSI SAF (2022): Product User Manual for Atlantic High Latitude level 3 Radiative Flux, EUMETSAT SAF on Ocean and Sea Ice. https://osi-saf.eumetsat.int/products/radiative-fluxes-products

1.3. Scope of this document

This Algorithm Theoretical Baseline Document presents the Atlantic High Latitude (AHL) Level 3 Radiative Flux products from the EUMETSAT Ocean and Sea Ice Satellite Application Facility (OSI SAF). The focus of this document is to present a short overview of how these products are produced and describe technical details about the products format to enable users to understand and use the products.

1.4. Overview

The high latitude radiative flux products have been produced since 2002. In the start the products were merged with the low/mid latitude products for a complete Atlantic coverage. Since 2011 the high latitude products have been distributed separately, as OSI-301 for DLI and OSI-302 for SSI. OSI-301 and OSI-302 are daily products in 5km resolution, based on orbit data gridded to fixed tiles before cloud masking and processing.

This ATBD describes the updated version of the products, labelled OSI-301-c and OSI-302-c. The major changes for this update are:

- Including NPP and NOAA-20 VIIRS data
- Including Metop-C AVHRR data (no longer using Metop-A)
- Replacing the cloud type product from PPS v2014 with v2021.

1.5. Reference and applicable documents

1.5.1. Reference documents

[RD.1] EUMETSAT OSI SAF
Scientific Validation Report for Atlantic High Latitudes level 3 Radiative Flux products
SAF/OSI/CDOP3/MET-Norway/SCI/RP/372, version 2.1, 07.01.2022

[RD.2] EUMETSAT OSI SAF
PUM for Atlantic High Latitudes level 3 Radiative Flux products.
SAF/OSI/CDOP3/MET-Norway/TEC/MA/373, version 2.1, 05.01.2022

1.5.2. Applicable documents

[AD.1] EUMETSAT OSI SAF
Product Requirements Document
SAF/OSI/CDOP3/MF/MGT/PL/2-001, version 1.9, 31.12.2021

[AD.2] EUMETSAT OSI SAF
Service Specification Document
SAF/OSI/CDOP3/MF/MGT/PL/003, version 1.12, 31.12.2021

1.6. Glossary

Acronym	Description
AHL	Atlantic High Latitudes
AVHRR	Advanced Very High Resolution Radiometer
DLI	Downward Longwave Irradiance
ECMWF	European Centre for Medium range Weather Forecasts
HL	High Latitudes
NetCDF	Network Common Data Form
NOAA	National Oceanic and Atmospheric Administration
NWC SAF	Nowcasting SAF
NWP	Numerical Weather Prediction
OSI SAF	Ocean and Sea Ice SAF
PPS	Polar Processing System
SAF	Satellite Application Facility
SSI	Solar Surface Irradiance
VIIRS	Visible Infrared Imaging Radiometer Suite

2. Input data

The radiative fluxes are retrieved from AVHRR data collected by Metop-C, Metop-B and NOAA-19 satellites, and VIIRS data from NPP and NOAA-20 satellites. The processing is done on the original satellite swath. The input data required for OSI-301-c and OSI-302-c differs and are specified below.

2.1. Surface Solar Irradiance

The AVHRR and VIIRS data used are bi-directional reflectance and observation geometry:

- R06 – bi-directional reflectance around 0.6μm
- R09 – bi-directional reflectance around 0.9μm
- SAZ – Satellite zenith angle
- SOZ – Solar zenith angle
- RAZ – relative azimuth angle between satellite and Sun.

The auxiliary data used are:

- *Combined land/sea mask and topography model* - GTOPO30 from USGS
- *Monthly climatology of surface albedo* over land. These are broadband albedo with Sun at zenith developed by Csizar and Gutman (1999).

- *Monthly climatology of ozone* from Total Ozone Mapping Spectrometer. These data are collected from a climatology estimated for the period 1979 – 1992
- *Predicted integrated water vapour content* in the atmosphere from a NWP model (NWC SAF PPS field)
- *Cloud type* from NWC SAF PPS v2021, that gives also information on the snow cover in case of clear sky or high semi-transparent clouds
- Cloud type conditions (Common geophysical and processing conditions flag) from NWC SAF PPS v2021
- *Sea ice cover* from the OSI SAF project, using the sea ice edge product (OSI-402-d).

2.2. Downward Longwave Irradiance

The input data are OSI-302-c when those are available and of good or excellent quality, and NWC SAF PPS data.

The auxiliary data used are:

- *Combined land/sea mask and topography model* - GTOPO30 from USGS.
- *Monthly climatology of surface albedo* over land. These are broadband albedo with Sun at zenith developed by Csizar and Gutman (1999).
- *Monthly climatology of ozone* from Total Ozone Mapping Spectrometer. These data are collected from a climatology estimated for the period 1979 – 1992 and is given in cm.
- *Predicted integrated water vapour content, surface temperature, surface pressure, and 2m relative humidity* in the atmosphere from a NWP model (NWC SAF PPS fields).
- Cloud type from NWC SAF PPS v20121, that gives also information on the snow cover in case of clear sky or high semi-transparent clouds
- Cloud type conditions (Common geophysical and processing conditions flag) from NWC SAF PPS v2021
- *Sea ice cover* from the OSI SAF, using the sea ice edge product (OSI-402-d).
- SOZ – Sun zenith angle: used only to set the confidence flag

3. Algorithms

3.1. Surface Shortwave Irradiance

3.1.1. Introduction

The solar irradiance at the surface is a function of the solar irradiance at the top of the atmosphere, the clear sky atmospheric transmittance and the cloud transmittance:

$$\begin{aligned} E &= S' \mu_0 T_a T_c \\ S' &= \frac{S_0}{\rho^2} \\ \mu_0 &= \cos\sigma \end{aligned} \tag{1}$$

where σ is the solar zenith angle, S_0 is the solar constant (1358 W/m^2 when band weighted). ρ^2 is a correction factor for the varying distance between the earth and the Sun and is given in chapter 3.1.3 below.

The clear sky transmittance (T_a) is not dependent on the satellite observation, it is merely a function of solar zenith angle and atmospheric load of water vapour, ozone, and aerosol and the surface albedo.

The cloud transmittance (T_c) is a function of the cloud albedo and requires several processing steps (see below).

3.1.2. Equations for clear sky transmittance

This clear sky parametrization is described in Darnell et al. (1988) and Darnell et al. (1992). The clear sky atmospheric transmittance (T_a) is estimated as a function of absorption in water vapour, ozone, oxygen, and carbon dioxide, scattering by aerosols and Rayleigh scattering. The atmospheric backscatter is parametrized by the surface pressure and albedo:

$$\begin{aligned} T_a &= e^{-\tau}(1+0.065\, p_s A_s) \\ \tau &= \tau_0 \left(\frac{1}{\mu_0}\right)^N, \text{where } N = 1.1 - 2\tau_0 \\ \tau_0 &= \tau_{O3} + \tau_{H2O} + \tau_{CO2} + \tau_R + \tau_a \\ \tau_{O3} &= 0.038 U_{O3}^{0.44} \\ \tau_{H2O} &= 0.104 U_{H2O}^{0.3} \\ \tau_{O2} &= 0.0076 p_s^{0.29} \\ \tau_R &= 0.038 p_s \\ \tau_a &= 0.007 + 0.009 U_{H2O} \end{aligned} \tag{2}$$

In the equations above, τ represents the optical depth due to various absorbers, μ_0 is as before the cosine of the solar zenith angle, p_s is the nominal surface atmospheric pressure in atmospheres and U

is the atmospheric load (in cm) of various constituents. In our algorithm implementation p_s is simplified as a constant equal to 1 atm.

3.1.3. Equations for cloud transmittance

a) Calibration

Adapting the procedure described by NOAA/NOAASIS and described by Rao and Chen (1996, 1999) at the NOAASIS home page, the digital counts is converted to scaled radiance or often called albedo using a standard linear relationship for the visible channels (NOAA-14 and prior, split-gain for successors). Using the nomenclature of NOAA the "albedo" or better - "reflectance factor" or "scaled radiance" is given as:

$$A = SC_{10} + I \tag{3}$$

where C_{10} is the 10-bit count value, S and I are the slope and intercept. The basic processing of AVHRR and VIIRS data at MET Norway provides A.

The equation above gives the reflectance factor for overhead sun. However, the annual cycle in the extraterrestrial solar irradiance is approximately $\pm 3\%$ about the mean due to a variation in the distance between the earth and the Sun. This variation can be defined in different ways, the implementation at MET Norway follows the specification of Paltridge and Platt (1976).

$$\rho^2 = \frac{1}{1.00011 + 0.034221\cos\theta + 0.001280\sin\theta + 0.000719\cos 2\theta + 0.000077\sin 2\theta} \tag{4}$$

where

$$\rho^2 = \frac{D^{SE}}{\overline{D^{SE}}} \quad \text{and} \quad \theta = 0.9863 d_n = \frac{2\pi d_n}{365}$$

D^{SE} is the actual distance between the Sun and the Earth and $\overline{D^{SE}}$ is the mean distance (referring to 1AU). d_n is the Julian Day of the year starting at 0 on January 1 and ending at 364 on December 31. In the equation for θ above the last statement produces output in radians and the first in degrees.

Using the information above, the processing of bi-directional reflectances r for input the SSI estimation at MET Norway is performed using:

$$r = \frac{\rho^2 A}{\cos\theta_0} \tag{5}$$

where A is the standard scaled radiance. r is first in the range 0-100 but is transformed to the range 0-1 before it is used to estimate the cloud transmissivity.

b) Narrowband to Broadband corrections

The NOAA/AVHRR NTOB correction scheme described by Hucek and Jacobowitz (1995) for Atlantic Ocean (Ocean 2 in Table I below) is used. The regression coefficients are used in a formula of the type:

$$r_b = a + b_1 r_1 + b_2 r_2 \quad (6)$$

where r_1 is the 0.6um reflectance and r_2 is the 0.9um channel reflectance, r_b is the broad band reflectance and a, b_1 and b_2 are coefficients provided in Table I.

Here, the cloud cover is obtained from the cloud classification as indicated in chapter 5. The coefficients for the land, ocean and snow surface types are used. The other surface types are not used.

If there is sea-ice (OSI SAF sea ice product used), or if there is snow indicated in the cloud type classification (detectable only if clear sky or fragmented clouds conditions) the coefficients over snow are chosen. If it is cloudy (except for fragmented clouds), the presence of snow over land is not known. In this case we only know if we are over land or sea using the landmask.

Coefficient	Surface type						
	snow 1	ocean 2	land 3	desert 4	land 5	ocean 6	coast 7
Clear							
a	**3.8995**	**1.78**	**2.17**	**2.60**	**2.95**	**2.34**	**2.77**
b_1	**0.0520**	**1.3302**	**0.3999**	**0.3896**	**0.2331**	**1.2062**	**0.3779**
b_2	**0.7423**	**-0.6250**	**0.4333**	**0.3873**	**0.5025**	**-0.5504**	**0.4168**
Partly cloudy							
a	*-0.1174*	**4.11**	**4.24**	**3.12**	**3.27**	**5.38**	**4.65**
b_1	*-0.0650*	**0.9029**	**0.3166**	**0.2705**	**0.2063**	**0.8909**	**0.3085**
b_2	*0.8671*	**-0.2441**	**0.3948**	**0.4811**	**0.4926**	**-0.2876**	**0.3856**
Mostly cloudy							
a	*-0.1174*	**5.08**	**4.75**	**5.49**	**9.53**	**8.51**	**5.36**
b_1	*-0.0650*	**0.4711**	**0.3757**	**0.3255**	**0.2844**	**0.3664**	**0.4362**
b_2	*0.8671*	**0.2983**	**0.3870**	**0.3961**	**0.3149**	**0.3308**	**0.3227**
Overcast							
a	**-0.1174**	**8.19**	**6.98**	**7.50**	**13.28**	**13.72**	**7.79**
b_1	**-0.0650**	**0.2301**	**0.2566**	**0.7564**	**0.2998**	**0.0076**	**0.2930**
b_2	**0.8671**	**0.5032**	**0.4907**	**-0.0136**	**0.3530**	**0.6310**	**0.4446**

Table I: Regression coefficients from the Hucek and Jacobowitz (1995) model. The model depends on the surface type and cloud amount. When there is snow and it is partly or mostly cloudy, no values are given in Hucek and Jacobowitz (1995). The coefficients used here for this case (values in italic) are the same as those used in the overcast case.

This NTOB correction is for AVHRR data and is not suited to be used directly for VIIRS data. One way to solve this is to intercalibrate VIIRS data with AVHRR data to find the difference between the equivalent visible channels on the two instruments, that is channel 1 versus channel M5 (~0.6um) and channel 2 versus channel M7 (~0.9um) on AVHRR and VIIRS, respectively. This has been done by collocating pixel from Metop-B and NOAA-20 orbits that are close in time and finding pairs of pixel from the AVHRR and VIIRS instruments on the two satellites that are less separated less than 500m in space and 5min in time. Only collocations with satellite zenith angles less than 2 degrees were used, to have

the same atmospherical path lengths. Since the NTOB scheme is only used for cloudy condition, the collocations were also restricted to only cases were both pixels were classified as cloudy by the PPS cloud mask. By looking at the fractions between the two equivalent channels, correction factors can be calculated that can be applied to the intercalibrate the two sets of channels. The results are shown in Figure 1, and the median values of the two distributions shown in the figure are used as correction factors.

The equations for calculating the corrected 0.6um and 0.9um VIIRS reflectances ($r06_{corr}$, $r09_{corr}$) before they are applied in the NTOB correction is therefore

$$r06_{corr} = 0.8510 * r06$$
$$r09_{corr} = 0.6948 * r09$$

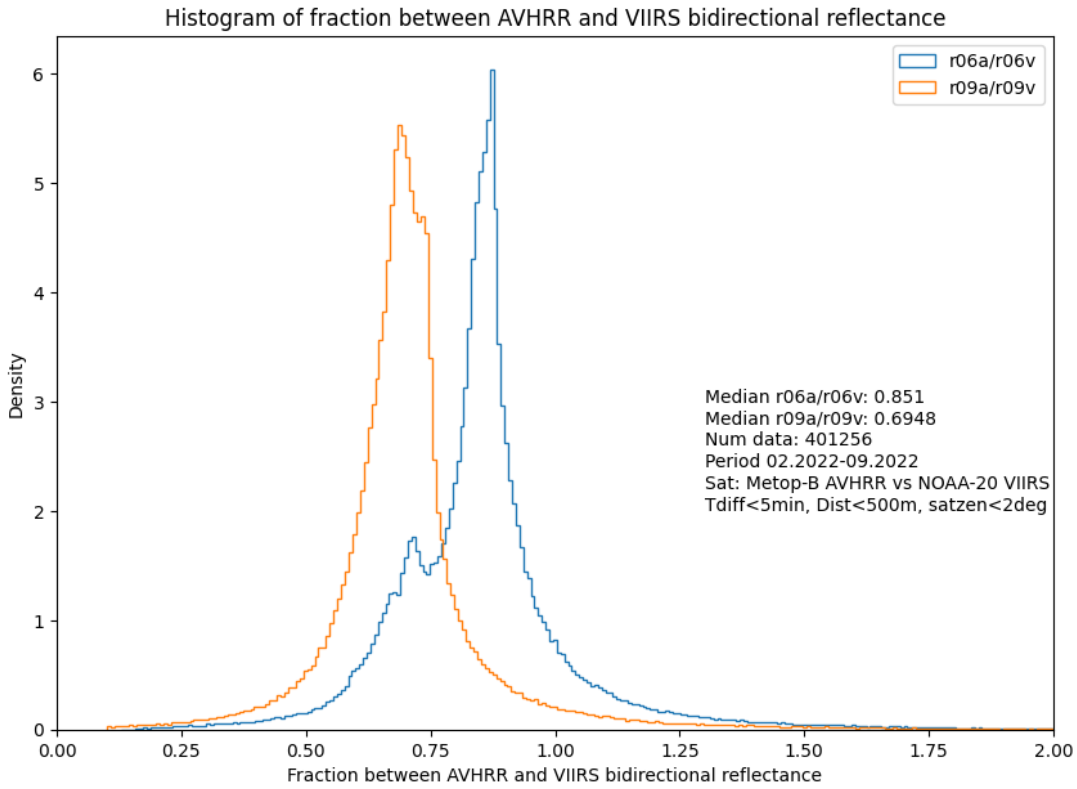

Figure 1: Histogram of fraction between equivalent bands on AVHRR and VIIRS for data between Febrary and September 2022. In blue is shown AVHRR channel 1/VIIRS channel M5 (~0.6um) and in orange AVHRR channel 2/VIIRS channel M7 (~0.9um).

c) Anisotropy correction

The broadband bi-directional reflectance is converted to albedo (planetary) by the method described in Manalo-Smith et al. (1998).

If the surface is not isotropic it is said to be anisotropic and the degree of anisotropy is described by the Bi-Directional Reflectance Function (BRDF) *R* or anisotropic factor[1]:

$$R(\theta,\varphi,\sigma)=\frac{\pi L(\theta,\varphi,\sigma)}{M} \tag{7}$$

where θ is the satellite zenith angle, φ the relative azimuth angle and σ is the solar zenith angle. If *R* is close to unity the assumption of isotropic reflection is not all wrong.

The relationship between the bi-directional reflectivity (*r*) and the albedo (a) is given by:

$$a(\sigma)=\frac{R(\theta,\varphi,\sigma)}{r(\theta,\varphi,\sigma)} \tag{8}$$

In practice, the bi-directional reflectivity is affected by the cloud cover and the surface types. It depends on empirical coefficients described in Manalo-Smith et al. (1998). So far the bi-directional reflectivity we use here it is only fully adapted for ocean surfaces, and it takes into account if it is clear sky, partly covered, or overcast, according to the cloud classification given in chapter 5.

d) Cloudy sky parametrization

The cloud transmittance (T_c) is estimated according to the equations specified by Frouin and Chertok (1992). Using the albedo at top of the atmosphere, a combined cloud and surface albedo is estimated. The difference between this combined albedo and the surface albedo can be related to the cloud absorption. Cloud absorption and the combined surface and cloud albedo are used to estimate the cloud transmittance. The equations used are given below:

$$\begin{aligned} A &= A_{ray}+\frac{T_{dt}A'}{1-S_aA'} \\ a_c &= m\mu_0(A'-A_s) \\ T_c &= \frac{1-A'-a_c}{1-S_aA'} \end{aligned} \tag{9}$$

where A' is the cloud-surface albedo, a_c is the cloud absorption, A_s is the surface albedo adapted for the solar zenith and the surface type and m = 0.2. The surface albedo is computed using the approach of Csizsar and Gutman (1999) over land (independent from the cloud cover), using Briegleb et al. (1986) if over the ocean in clear sky conditions, and is taken as 6% if over the ocean and it is cloudy (diffusive downward irradiance). The parametrization we use neglects the snow effect except above permanent snow where the surface albedo is taken as 60%.

The atmospheric transmittances used above are given below:

1 Not to be confused with the reflectance factor or bi-directional reflectance as *R* is often used for this as well, *r* is used for this in this document.

$$\begin{aligned}
\tau_d &= \tau_{O3} U_{O3} (1/\mu_0 + 1/\mu) + \tau_{H2O} U_{WV} (1/\mu_0 + 1/\mu) + \tau_{sc} (1/\mu_0 + 1/\mu) \\
\tau_{dt} &= \tau_{O3} U_{O3} (1/\mu_0 + 1/\mu) + \tau_{H2O} 0.3 U_{WV} (1/\mu_0 + 1/\mu) + \tau_{sc} (1/\mu_0 + 1/\mu) \\
T_d &= e^{-\tau_d} \\
T_{dt} &= e^{-\tau_{dt}}
\end{aligned} \tag{10}$$

where U represents the atmospheric load of the specified substance in cm. T_d represents the transmittance Sun - Surface -Satellite and T_{dt} the transmittance Sun - Cloud - Satellite. The optical depth (τ) due to atmospheric constituents required above are given by:

$$\begin{aligned}
\tau_{H2O} &= 0.102 (U_{WV}/\mu_0)^{0.29} \\
\tau_{O3} &= 0.041 (U_{O3}/\mu_0)^{0.57} \\
\tau_{sc} &= (a + b/V)\mu_0 \\
&maritime: a = 0.059\, b = 0.359\, a' = 0.089\, b' = 0.503 \\
&continental: a = 0.066\, b = 0.704\, a' = 0.088\, b' = 0.456
\end{aligned} \tag{11}$$

τ is still the optical depth due to various absorbers. τ_{sc} is scattering due to both Rayleigh and molecules.

3.1.4. Daily integration

The daily estimate of the SSI is performed by a straightforward arithmetic mean according to:

$$\overline{SSI} = \sum_{i=1}^{N} w_i^{time} K_i SSI^{clear} \tag{12}$$

where

- w is a temporal weight to handle to irregularly time spacing of polar orbiting data. This temporal weight if for the moment simplified and taken as 1. This way does not take into account the irregularities of the observations throughout the day some time periods might be represented by very few observations while other are well covered or over-represented. The absence of data during the night is not an issue as SSI^{clear} is null at night.
- SSI^{clear} is the mean clear sky irradiance computed this way :

$$SSI^{clear} = \int_{1day} SSI^{clear}(t) \approx \sum_{t_i = 0\,h}^{23\,h} SSI_i^{clear}(t_i)/24,$$

where t_i is discrete and takes values every hour from 00h to 23h. Each hourly clear sky value is computed on the entire grid and uses as requires hourly integrated water column vapour value (from NWP).

- K_i is the clearness index, estimated by:

$$K_i = \frac{SSI_i^{est}}{SSI_i^{clear}} \tag{13}$$

The concept of the weighting by K_i is illustrated in Figure 2. Basically the weights are similar to clearness indices which are applied to each clear sky estimate during the day.

Figure 2 Weighting of observations to estimate daily fluxes are performed according to the daily cycle of insolation.

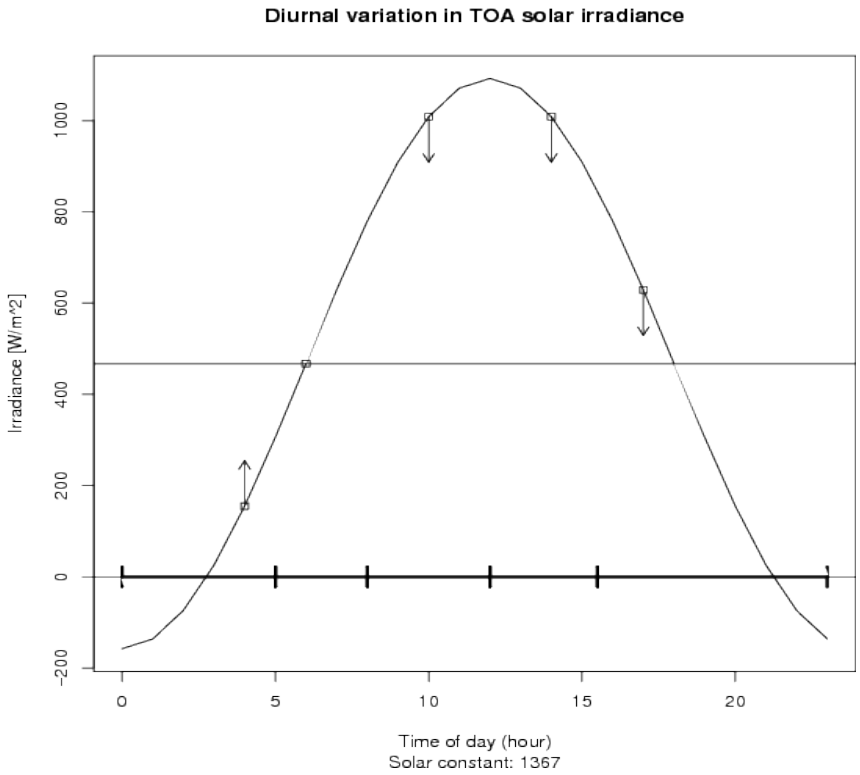

3.2. Downward Longwave Irradiance

3.2.1. Method and equations

According to experience gained developing algorithms for Low and Mid Latitude within the OSI SAF (Brisson et al., 2000) a hybrid method was chosen for estimation of DLI. This is a combination of a bulk parametrization and a satellite derived cloud amount. Basis for the method is briefly described in Godøy (2004) and by the equations below.

DLI is estimated using Stefan-Boltzmann law, a clear sky emissivity (ε_0) and a cloud contribution coefficient (C) :

$$L = (\epsilon_0 + (1-\epsilon_0)C)\,\sigma\,T_a^4$$

ϵ_0 : *clear sky emissivity*

C : *infrared cloud amount*

σ : *Stefan − Boltzman constant* $(5.6696\times10^{-8}\,\frac{W}{m^2\,K^4})$

T_a : *Air temperature* $(Kelvin)$

(14)

Basically the DLI is a sum of the clear sky emitted irradiance (first term), the contribution from cloud (second term) and minus the clear sky contribution obscured by clouds.

The main challenge is to determine the method to use for the clear sky emissivity, how to determine the cloud amount and how to actually implement the method in practice.

To estimate the clear sky emissivity the formulation of Prata (1996) specified in the equations below can be used. It rely on NWP model inputs.

$$\epsilon_0 = 1-(1+\xi)\exp[-\sqrt{(1.2+3.0\xi)}] - 0.05\,\frac{(p_0-p)}{(p_0-710)}$$

p_0 : $1013.25[hPa]$

(15)

$$\xi = c\left(\frac{e_0}{T_a}\right)$$

where e_0 *is surface water vapor pressure ,* c *is* $46.5[\frac{cm\,K}{hPa}]$

(16)

As the method of Prata needs the surface water vapour pressure (e_0) as input this is estimated using the product of the saturation water vapour pressure *(e_s)* and relative humidity *(R_h). e_s* is estimated using the Goff- Gratch equation (below) (Goff and Gratch, 1946, List, 1984). The two equations below are for the saturation water vapour pressure over plane surfaces of water and ice.

$$\begin{aligned}
&If\ T_a > 273.15\ use:\\
&e_s = 10^{(23.8319 - 2948.964/T_a - 5.028\log_{10}T_a - 29810.16\exp(-0.0699382T_a) + 25.21935\exp(-2999.924/T_a))}\\
&If\ T_a < 273.15\ use:\\
&e_s = 10^{(2.07023 - 0.00320991T_a - 2484.896/T_a + 3.56654\log_{10}T_a)}
\end{aligned}$$

(17)

Concerning the cloud contribution, at least two different methods can be used.

a) Cloud contribution by bulk parametrization coming from pyrgeometer observations

The cloud contribution can be estimated by summarizing individual cloud contribution coefficients and the fractional cloud cover.

$$C = \sum_i (n_i C_i)$$
$$C_i : contribution\ coefficient\ by\ cloud\ type\ i$$
$$n_i : fractional\ cloud\ cover\ by\ cloud\ type\ i \quad (18)$$

The cloud types we differentiate are shown in Table II. Brisson et al (2000) showed that cloud contribution coefficients can be estimated using surface pyrgeometer observations according to the equation below.

$$C_i = \frac{(L_m - \epsilon_0 \sigma T_a^4)}{[(1-\epsilon_0)\sigma T_a^4]} \quad (19)$$
$$L_m : Observed\ downward\ longwave\ irradiance$$

Given a classified satellite image (e.g. Nowcasting SAF PPS products, Dybbroe et al., 2000) a contribution coefficient can be estimated for each cloud type represented in the classified image.

b) Cloud contribution using SSI values

Brisson et al (2000) also presented another method that can be used to infer *C*. This method (see below) is only applicable during day time and is based upon use of the SSI product (e.g. Godøy and Eastwood, 2002a, 2002b).

$$C = 1 - \frac{E}{E_{clr}} \quad (20)$$
$$where\ E\ is\ the\ estimated\ surface\ solar\ irradiance\ (SSI)\ using\ AVHRR\ data,$$
$$E_{clr}\ is\ the\ clear\ sky\ calculated\ SSI$$

In this equation the infrared cloud amount is directly related to the optical thickness of the cloud. The closer the satellite observed SSI is to the clear sky, the less contribution from cloud in the DLI estimate. This method is used if all the following conditions are fulfilled: the confidence level for SSI is good or excellent, the solar zenith angle is lower than 80 degrees, there is no twilight, no sunglint and the cloud cover does not have a low level inversion.

Daily integration of the DLI product is easier than for the SSI product as there is no diurnal cycle to specifically handle. The daily integration is implemented by a straightforward arithmetic mean where each individual observation throughout the day is representative for a time period. This way does not take into account the irregularities of the observations throughout the day. Some time periods might be represented by very few observations while other are well covered or over-represented.

4. Processing overview

This section describes the processing scheme used for HL SSI products. AVHRR and VIIRS data are processed whenever they are available, resulting in instantaneous (passage) SSI and DLI estimates. The instantaneous estimates are combined into a daily product

4.1. Processing SSI and DLI on satellite swaths

The radiative fluxes are computed on the satellite swath (Figure 3 and Figure 4) for each satellite passage: all the inputs enumerated in 2.1 and 2.2 need to be sampled on the swath geometry. The monthly climatology of the albedo and ozone, as well as the ice cover are resampled on the satellite swath using a nearest interpolation using the pyresample package in Python. The other data are provided on swath (for example by NWC SAF PPS v2021) or are directly computed for each point of the swath.

Figure 3: Example of SSI on swath. Retrieved from NOAA 19 (2018/08/30 12:48-13:13)

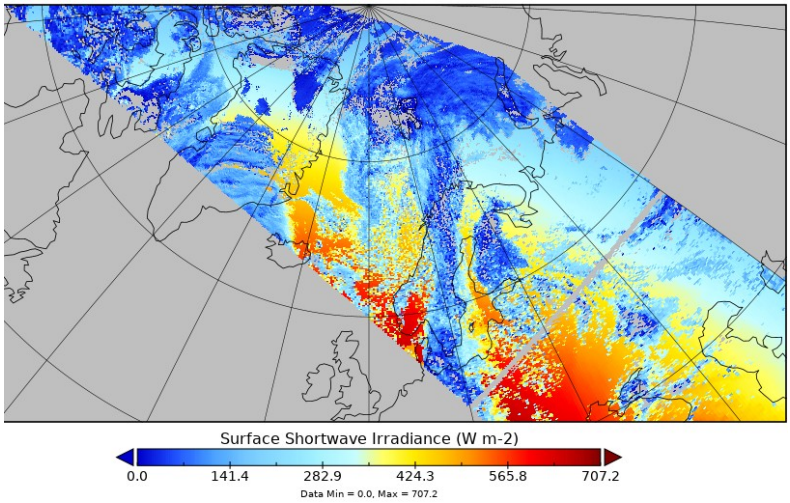

Figure 4: Example of DLI product on swath (Retrieved from NOAA 19 (2018/08/30 12:48-13:13)

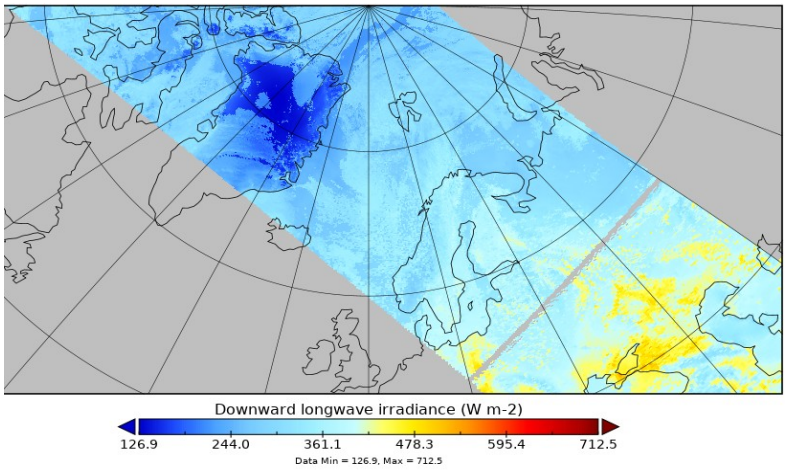

4.2. Surface Solar Irradiance

The instantaneous processing of AVHRR and VIIRS data is presented in Figure 5. It uses the algorithms described in 3.1 using the input data described in 2.1.

Figure 5: Flowchart for processing of passage data to SSI.

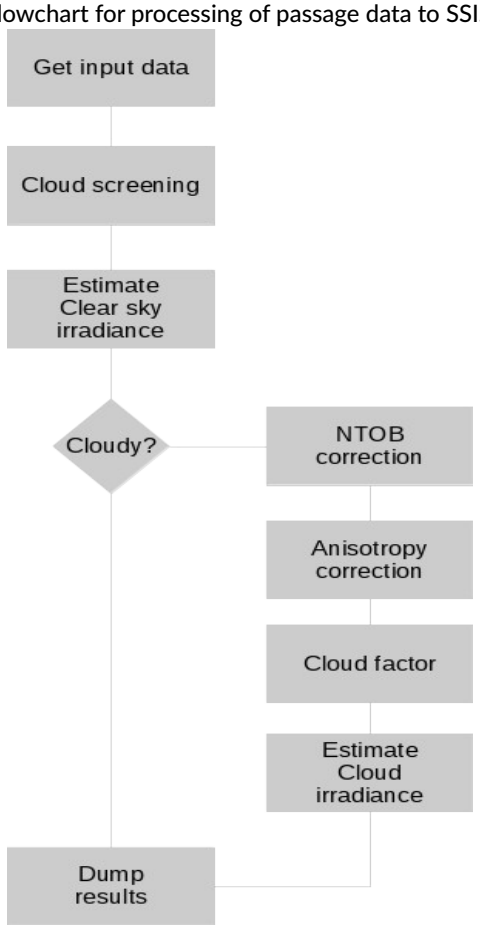

4.3. Downward Longwave Irradiance

This section describes the processing scheme used for HL DLI products. AVHRR and VIIRS data are processed whenever they are available, resulting in instantaneous DLI estimates. The instantaneous processing of AVHRR and VIIRS data is presented in Figure 6. It uses the algorithms described in 3.2 using the input data described in 2.2.

Figure 6: Flowchart for processing of passage data to DLI.

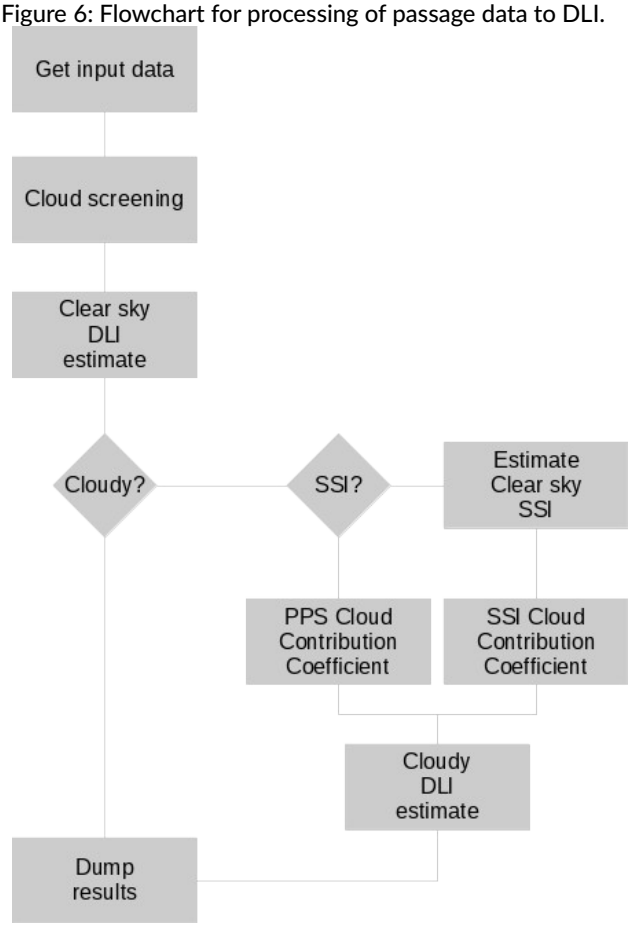

4.4. Resampling on a grid

The radiative flux products obtained on swaths are then resampled to a polar stereographic map projection with 5 km grid resolution. For SSI, DLI and the column water vapour, this is done by using the 50 nearest neighbour in a 2.5 km radius, and these values are equally weighted. During the gridding process of SSI/DLI only the data which have confidence levels as excellent, good or acceptable are kept. The map projected passage products are then averaged into daily products in the same map projection, i.e. the OSI SAF Atlantic High Latitude DLI (OSI-301-c) and SSI (OSI-302-c) products.

4.5. Daily estimate of SSI and DLI

The estimation of daily SSI values (Figure 7) is based on the combination of temporally irregularly spaced observations using weights (Equations 12 and 13). The weight The daily DLI (Figure 8) is a straightforward average.

Figure 7: Example of daily SSI product 2018/08/30)

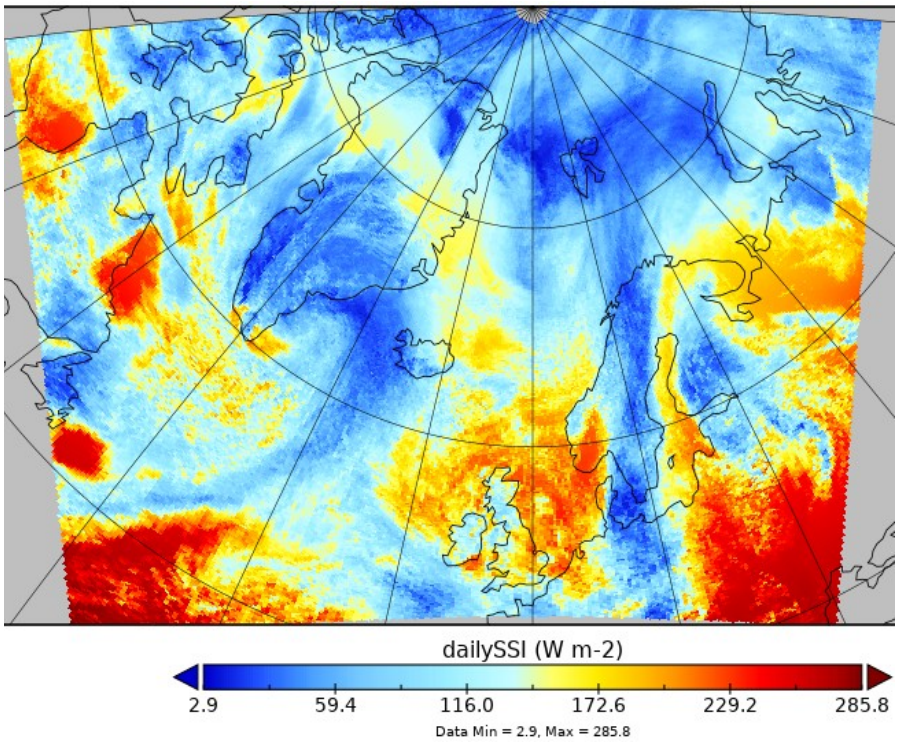

Figure 8: Example of daily DLI product 2018/08/30

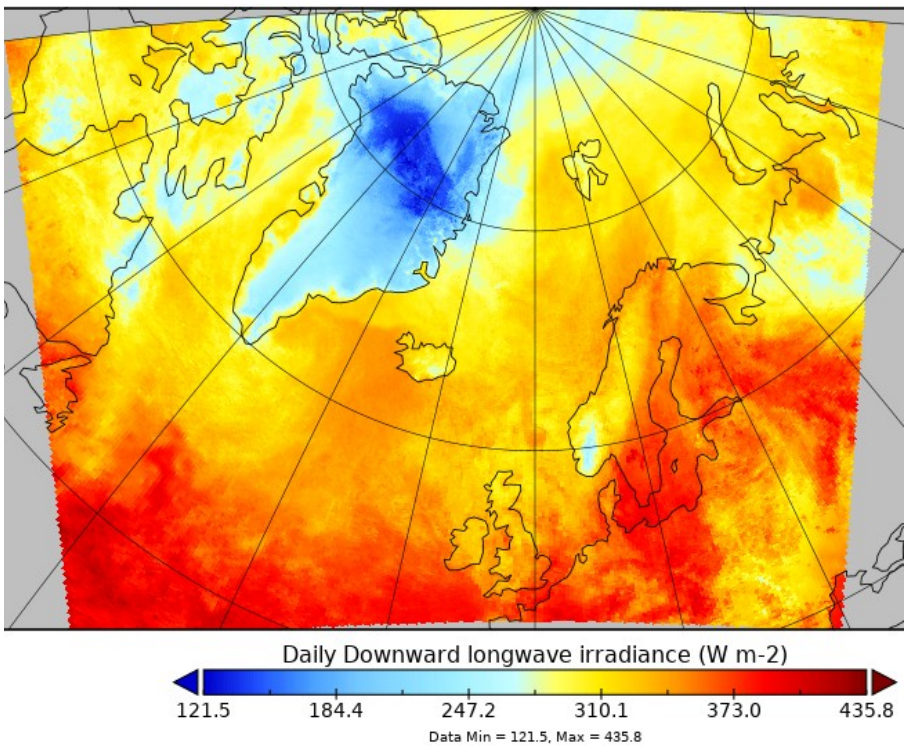

4.6. Confidence levels

Each DLI or SSI pixel value is associated to a confidence level expressed on a scale with 6 values:

0 : unprocessed, 1 : erroneous, 2: bad, 3: acceptable, 4: good, 5 : excellent.

The 0 value corresponds most of the time to space or missing data, and, for SSI, to a solar zenith angle (SOZ) larger than 80 degrees. The 1 value corresponds to an error in the algorithms or software logic. The other value meanings depend on the products and are described below. When attributing the confidence levels, the conditions are checked from the worse level to the best level, and a given confidence level cannot be attributed if conditions for lower confidence levels are met.

4.6.1. SSI

The single passage SSI confidence levels are defined as follows:

- Excellent - cloud factor between 0 and 1 and consistent with cloud cover (rules for consistency given below), this is never used for partly cloud contaminated pixels.
- Good - no sunglint and cloud factor between 0.2 and 1 and not fully consistent with cloud cover, or fractional cloud conditions.
- Acceptable - clear sky, cloud factor equals 0 and is consistent with cloud cover or cloud factor equals 1 (regardless of consistency), or sunglint and fractional clouds, or sunglint and cloud factor equals 0.
- Bad - low cloud factor and inconsistent with cloud cover.
- Erroneous - error in NTOB or BRDF or clear sky insolation or cloud transmittance.
- Unprocessed - out of area, night, or SOZ>80 degrees.

Each single SSI passage is then resampled to a polar stereographic map projection with 5 km grid resolution. The pixels of the single passage SSI data are used in the resampling process only if their confidence levels are equal or better than acceptable. The confidence level associated to the resampled SSI value (on grids) is set so that at least 99% of the passage pixels used to obtain this value have an equal or better confidence level than the one which is finally set. During the final daily averaging, the confidence levels of the gridded products are averaged and rounded to the nearest confidence level.

4.6.2. DLI

The single passage DLI confidence levels are defined as follows:

- Excellent - using SSI of excellent confidence level and no night, sunglint or twilight in the cloud type conditions and no low level quality inversion of the cloud type. When SSI is not used (bulk parametrization), and the solar zenith angle is lower than 80 degrees.
- Good - using SSI of good confidence level together with no night, sunglint or twilight in the cloud type conditions and no low level quality inversion of the cloud type.
- Acceptable - when using bulk parametrization and low or medium level cloud types are found together with a less than 80 degrees solar zenith angle and together with one of the following conditions: bad or questionable quality of the cloud type, or low level inversion of the cloud type, or reclassified cloud type. Or when solar zenith angle is higher than 80 degrees.

- Bad - when using bulk parametrization and low or medium level cloud types are found together with an over 80 degrees solar zenith angle and together with one of the following conditions : bad or questionable quality of the cloud type, or low level inversion of the cloud type, or reclassified cloud type. When using bulk parametrization and the cloud type is not defined.
- Erroneous – no cloud type or failure in DLI computations (ex: failure in cloud contribution).
- Unprocessed - out of area.

The confidence level for daily products is found by averaging the single passage DLI estimates averaged to the AHL grid (5 km). Only pixels with confidence level equal to or better than acceptable (3) are used in the average. The confidence level associated to the resampled DLI value (on grids) is set so that at least 99% of the passage pixels used to obtain this value have an equal or better confidence level than the one which is finally set. During the final daily averaging, the confidence levels of the gridded products are averaged and rounded to the nearest confidence level.

5. Appendix on the cloud classification

The OSI SAF HL cloud type generation is performed using the NWC SAF PPS v2021 cloud type software. This software generates the cloud types shown in Table Table II. However, the SSI and DLI estimation does not need all these classes, thus subsets of cloud types are used. The relation between the original cloud types and the subsets used in the SSI and DLI estimations is shown this table.

#	Cloud category SAF NWC PPS	Simplified classification used to compute the cloud contribution (for DLI)	Simplified classification used in NTOB corr. (for SSI)	Scene info used in NTOB corr (for SSI)	Cloud cover used in BRDF (for SSI)
1	Cloud free land	Clear	Clear		0%
2	Cloud free sea				
3	Land contaminated by snow			Snow	
4	Sea contaminated by snow/ice			Snow	
5	Very low clouds	Low clouds	Overcast		100%
6	Low clouds				
7	Medium level clouds	Medium level clouds	Overcast		100%
8	High opaque clouds	High opaque clouds	Overcast		100%
9	Very high opaque clouds				
10	Fractional or subpixel cloud	Fractional clouds	Mostly cloudy		50%
11	High semi-transparent very thin cirrus cloud	Thin cirrus	Overcast		100%
12	High semi-transparent thin cirrus cloud				
13	High semi-transparent thick cirrus cloud	Thick cirrus	Overcast		100%
14	High semi-transparent cirrus above low or medium level cloud				
15	High semi-transparent above snow/ice		Overcast	Snow	100%
255	No-Corrupted data	NA	NA	NA	NA

Table II: Cloud classification given by NWC SAF PPS-v2021. SSI and DLI estimates depend simplified cloud cover classifications, and on the presence of snow. The cloud type and cloud conditions are for example used in the NTOB correction and to evaluate BRDF.

6. References

Brisson, A., P. Le Borgne, and A. Marsouin, 2000: Development of algorithms for Downward Longwave Irradiance retrieval at O&SI SAF Low and Mid Latitudes, Project Report O&SI SAF Low and Mid Latitudes, Meteo-France/SCEM/CMS/, 22302 Lannion, France, February 2000.

Csizsar, I. and Gutman, G., 1999: Mapping global land surface albedo from NOAA AVHRR, JOURNAL OF GEOPHYSICAL RESEARCH, VOL. 104, NO. D6, PAGES 6215-6228, MARCH 27, 1999

Darnell, W.L., F. Staylor, S.K. Gupta, and F.M. Denn, 1988: Estimation of surface insolation using sun-synchronous satellite data, J. Climate, Vol. pp. 820-835, 1988.

Darnell, W.L., W.F. Staylor, S.K. Gupta, N.A. Ritchey, and A.C. Wilbur, 1992: Seasonal variation of surface radiation budget derived from international satellite cloud climatology project C1 data, J. Geophys. Res., Vol. 97, pp. 15 741 - 15760, 1992.

Dybbroe, A., K.-G. Karlsson, M. Moberg, and A. Thoss, 2000: Scientific report for the SAFNWC Mid Term Review, Swedish Meteorlogical and Hydrological Institute, SE-60176 Norrkøping, Sweden.

Dybbroe, A., Karlsson, K.-G., Thoss, A., 2005a: NWC SAF AVHRR cloud detection and analysis using dynamic thresholds and radiative modelling - Part I: Algoritm description. J. Appl. Meteor., 44, 39-54.

Dybbroe, A., Karlsson, K.-G., Thoss, A., 2005b: NWC SAF AVHRR cloud detection and analysis using dynamic thresholds and radiative modelling - Part II: Tuning and Validation. J. Appl. Meteor., 44, 55-71.

Frouin, R., and B. Chertok, 1992: A Technique for Global Monitoring of Net Solar Irradiance at the Ocean Surface. Part I: Model, J. Appl. Met., Vol. 31, pp. 1056-1066.

Godøy, Ø. And S. Eastwood, 2002a: Testing of short-wave irradiance retrieval algorithms under cloudy conditions, *DNMI Research Note No. 69*, ISSN 0332-9879, Norwegian Meteorological Institute, Oslo, Norway, 2002, 20pp.

Godøy, Ø., and S. Eastwood, 2002b: Narrowband to Broadband correction of NOAA/AVHRR data, *DNMI Research Note No. 69*, ISSN 0332-9879, Norwegian Meteorological Institute, Oslo, Norway, 2002, 12pp .

Godøy, Ø, 2004: Tuning and validation of a downward longwave irradiance retrieval algorithm, *Research Note No. 02/04 Remote Sensing,* ISSN 1503-8009, Norwegian Meteorological Institute, Oslo, Norway, 2004, 12pp

Godøy, Ø, 2005: Validation of the NWC SAF PPS cloud products, *Research Report No. 04/2005 Remote Sensing*, ISSN 1503-8025, Norwegian Meteorological Institute, Oslo, Norway, 2005, 14pp

Hucek, R., and H. Jacobowitz, 1995: Impact of Scene Dependence on AVHRR Albedo Models, J. Atm. Oce. Tech., Vol. 12, No. 4, pp. 697-711.

Karlsson, K.-G. and Dybbroe, A., 2010: Evaluation of Arctic cloud products from the EUMETSAT Climate Monitoring Satellite Application Facility based on CALIPSO-CALIOP observations. Atmos. Chem. Phys., 10, 1789-1807, doi:10.5194/acp-10-1789-2010, 2010

Liang, S., 2000: Narrowband to Broadband Conversion of land surface albedo: I Algorithms, Remote Sensing of Environment 76 (2000) 213-238.

Liang, S., Yu, Y., and Defilice, T.D., 2005: VIIRS narrowband to broadband land surface albedo conversion: formula and validation, International Journal of Remote Sensing Vol. 26, No. 5, 10 March 2005, 1019–1025

Manalo-Smith, N., G. L. Smith, S. N. Tiwari, and W. F. Staylor, 1998: Analytic forms of bi-directional reflectance functions for application to Earth radiation budget studies, J. G. R., Vol. 103, No. D16, pp. 19 733-19 751, 1998.

Paltridge, G.W., and C.M.R. Platt, 1976: Radiative processes in Meteorology and Climatology, Elsevier, ISBN 0-444-41444-4.

Posselt R., Mueller, R.W., Stöckli, R., and Trentmann, J., 2012: Remote sensing of solar surface radiation for climate monitoring — the CM-SAF retrieval in international comparison, Remote Sensing of Environment 118 (2012) 186–198, doi:10.1016/j.rse.2011.11.016.

Rao, C.N.R., and J. Chen, 1996: Post-launch calibration of the visible and near-infrared channels of the Advanced Very High Resolution Radiometer on the NOAA-14 spacecraft, Int. J. Rem. Sens., Vol. 17, pp. 2743-2747.

Rao, C.R.N, and J. Chen, 1999: Revised post-launch calibration of the visible and near-infrared channels of the Advanced Very High Resolution Radiometer (AVHRR) on the NOAA-14 spacecraft, Int. J. Rem. Sens., Vol. 20, No. 18, pp. 3485-3491.